JOURNAL OF GEOPHYSICAL RESEARCH, VOL. 107, NO. A10, 1305, doi:10.1029/2001JA000296, 2002

Ultraviolet insolation drives seasonal and diurnal space weather variations

Patrick T. Newell, Thomas Sotirelis, Joseph P. Skura, and Ching-I. Meng
Applied Physics Laboratory, Johns Hopkins University, Laurel, Maryland, USA

Wladislav Lyatsky
Center for Space Plasma and Aeronomic Research, Alabama A&M University, Normal, Alabama, USA

Received 10 September 2001; revised 2 January 2002; accepted 25 March 2002; published 17 October 2002.

[1] We present several findings that improve the understanding of the seasonal and diurnal variation in auroral and magnetospheric activity. The total ionospheric conductivity in the nightside auroral oval from UV insolation (Σ_P) is calculated, and its seasonal and diurnal variation is shown to correlate very highly with that of the Am and AL indices of geomagnetic activity (r = 0.89 and r = 0.75, respectively). Such excellent correlations with Am have been previously obtained by other researchers using instead the acute angle between the Earth's dipole axis and the Earth-Sun line, ψ. However, the ionospheric conductivity formulation provides a more physical model to explain the equinoctial (McIntosh) effect. Namely, the level of geomagnetic activity is well-ordered by whether the nightside auroral oval is sunlit in one hemisphere or neither. We improve calculations of the expected pattern of seasonal and diurnal variations in the solar wind input. The elliptical nature of the Earth's orbit results in observed interplanetary magnetic field (IMF) strengths about 7% larger in January than June. When the Sun's spin axis tilt to the ecliptic plane is considered, the predicted IMF southward component (Bs) maximizes in February, as is observed. We also calculate the seasonal and diurnal variation of a more general solar wind–magnetosphere coupling function, E_{KL}. E_{KL} proves to have little (0.5%) diurnal variation and has a seasonal variation of about 14%. For the first time, the seasonal and diurnal variation in the Φ_{PC}, the polar cap flux (from Polar UVI observations, cross-calibrated to a DMSP-based standard) and in magnetotail stretching (the b2i index) are presented. Magnetotail stretching proves to correlate better (r = −0.57) with E_{KL} than with Σ_P. Φ_{PC} correlates better with Σ_P, but the correlation (r = −0.49) is not nearly as strong as that for the indices of geomagnetic activity, Am and AL. Our survey of the seasonal and diurnal variation of the magnetosphere thus shows that some aspects (geomagnetic indices) correlate best with UV insolation, while others (magnetotail stretching) correlate best with solar wind input. *INDEX TERMS:* 2736 Magnetospheric Physics: Magnetosphere/ionosphere interactions; 2784 Magnetospheric Physics: Solar wind/magnetosphere interactions; 2704 Magnetospheric Physics: Auroral phenomena (2407); *KEYWORDS:* aurora, insolation, seasonal, magnetosphere, ionosphere, coupling

Citation: Newell, P. T., T. Sotirelis, J. P. Skura, C.-I. Meng, and W. Lyatsky, Ultraviolet insolation drives seasonal and diurnal space weather variations, *J. Geophys. Res.*, *107*(A10), 1305, doi:10.1029/2001JA000296, 2002.

1. Introduction

[2] It is well known that bright auroral displays occur most frequently around the equinoxes (see Figure 4.8 of *Chamberlain* [1961], based on work by Meinel, Negaard, and Chamberlain in 1954). Lately, it has become clear that most indices of geomagnetic activity also peak around equinoxes, and exhibit clear patterns of universal time (UT) variation as well [*Cliver et al.*, 2000; *Ahn et al.*, 2000]. The combined seasonal and diurnal variation of the AL and of the Am indices follows a well-defined pattern, with the amplitude of the UT variations around solstice reaching 37%. These large magnitude oscillations need to be understood before anything approaching a general understanding of space weather dynamics is possible.

[3] The equinoctial preference for geomagnetic activity was attributed by *Russell and McPherron* [1973] to the varying portion of the GSE IMF B_y which appears as a B_z component in the GSM coordinate system (GSE and GSM abbreviate Geocentric Solar Ecliptic and Geocentric Solar Magnetospheric, respectively). In fact the classical Russell-McPherron effect clearly is real. Elementary geometry and well-known effects of IMF-magnetosphere coupling imply

0148-0227/02/2001JA000296$09.00

it. Almost as clearly the Russell-McPherron effect does significantly affect the magnetosphere and auroral activity. Depending on whether the IMF points toward or away from the Sun, the average value of B_z can be either larger or smaller around either the spring or fall equinox.

[4] However, both toward and away IMF sectors structures are seen around both spring and fall. As a result, when averaged over all observed conditions, the actual excess of southward IMF expected or actually observed around equinoxes is too small in magnitude to account for more than a tiny portion of the statistical seasonal variation. Similarly, the annual variation in solar wind velocity cannot explain much of the equinoctial effect. Since the Sun's spin axis is tilted at 7.25° to the ecliptic, the heliographic latitude of the Earth varies over the course of a year, reaching its lowest latitude March 6, and highest September 8. As a result, the solar wind velocity observed at Earth varies by about 5–10% [*Zieger and Mursula*, 1998]. We believe it is quite clear that 5–10% variations in the magnitude of the solar wind velocity are not the primary explanation for the large seasonal variations observed. Indeed, both theoretical [*Perreault and Akasofu*, 1978; *Kan and Lee*, 1978; *Vasyliunas et al.*, 1982] and observational [*Wygant et al.*, 1983; *Liou et al.*, 1998] considerations overwhelmingly support a linear variation of geomagnetic and auroral activity with solar wind velocity. Seasonal variations in the incident solar wind velocity are thus a real but modest contributor to geomagnetic variations.

[5] Since so many effects are associated with the equinoxes, it is worthwhile to consider universal time variations as well, in any effort to unravel causation. *Cliver et al.* [2000] demonstrated that when the combined diurnal and seasonal effects are considered, the resulting patterns fit the Russell-McPherron effect even more poorly. Of course there is no diurnal variation in observed solar wind velocity – although the diurnal variations in geomagnetic activity are significant. *Cliver et al.* [2000] attributed the seasonal and diurnal pattern to a weaker efficiency of merging when the Earth's dipole axis is further from perpendicular to the Earth-Sun line. No physical motivation for that assumption was given.

[6] Meanwhile, *Newell et al.* [1996] demonstrated that intense discrete aurora are suppressed in sunlight. Confirmation soon followed by a variety of researchers. For example, the intense ion upflows associated with discrete aurora are least common in local summer [*Collin et al.*, 1998]. Auroral kilometric radiation is likewise stronger in winter than in summer [*Kasaba et al.*, 1997; *Kumamoto and Oya*, 1998], as are auroral electromagnetic ion cyclotron waves [*Erlandson and Zanetti*, 1998]. The suppression of intense nightside aurora by sunlight has also been confirmed from Polar ultraviolet [*Liou et al.*, 1998] and X-ray [*Petrinec et al.*, 2000] imagers.

[7] This strong summer hemisphere/winter hemisphere variation represents a seasonal effect which is quite distinct from the equinoctial effect, and provides further insights. Thus, *Newell* [1998] suggested that geomagnetic activity may maximize when the nightside oval of both hemispheres is in darkness, but did not then explore the suggestion further.

[8] *Lyatsky et al.* [2001] showed that, indeed, the combined seasonal and diurnal variation of the Am and AL indices could be reasonably well ordered by taking note of whether the nightside oval in one hemisphere was sunlit, or whether the nightside oval in both hemispheres was in darkness. Around equinoxes, of course, both nightside ovals are in darkness and auroral activity maximizes. At solstices, universal time variations are strongest. For example, in December or January the AL and Am indices minimize around 0300 UT when the Southern Hemisphere nightside oval is sunlit. Note that the *Lyatsky et al.* [2001] results using AL imply that geomagnetic in the Northern Hemisphere is not just suppressed during local sunlight, but is also reduced when the Southern Hemisphere nightside oval is sunlit. The key issue appears to be whether a conducting path for nightside field-aligned currents into the ionosphere is available in either hemisphere.

[9] The present paper makes several advances which we believe somewhat clarify the situation. First, we generalize the work of *Lyatsky et al.* [2001], who considered the solar zenith angle of the auroral oval at midnight, by calculating the global nightside ionospheric conductivity (that is, we add together southern and northern ionospheric conductivity, due to their parallel electrical pathways) due to solar illumination. The result is an extremely good fit to the seasonal and diurnal Am variations (r = 0.89) and a fairly good fit to AL variations (r = 0.75). Next, we generalize the Russell-McPherron effect in several ways, such as including the ellipticity of the Earth's orbit, and by considering a solar wind input function which is theoretically and empirically better supported (namely, the electric field $E_{KL} = vB_T\sin^2(\theta/2)$). The generalized Russell-McPherron effect so calculated correlates well with certain magnetospheric state variables, whose seasonal and diurnal variations are calculated here for the first time. Specifically, we show that the magnetotail stretching index, b2i, fits best to the generalized Russell-McPherron effect. We also calculate the seasonal and diurnal variations in polar cap size, as determined from Polar UVI (cross-calibrated to DMSP particle boundary standards). We thus are able to show that certain magnetospheric state variables, such as how stretched the magnetotail is, may depend mainly on the generalized solar wind input variations. However, indices of auroral activity, such as Am and AL fit much better to the global pattern of nightside auroral oval conductivity.

2. Generalizing the Ionospheric Conductivity Model

[10] Field-aligned currents originating in the magnetotail flow into, through, and back out of the ionosphere. Such field-aligned currents are in fact physically required by pressure gradients in the magnetotail [e.g., *Wing and Newell*, 2000]. Discrete aurora, including the substorm bulge, are always associated with field-aligned currents out of the ionosphere. When a conducting path into, through, and out of the ionosphere exists, this process of matching ionospheric capabilities to requirements imposed by the magnetosphere may proceed smoothly. However, when no conducting path exists, any patch of auroral precipitation will create some conductivity, which will then tend to draw more current. The result is an increase in the localized precipitation of electrons, and thus further enhancing the conductivity. *Atkinson* [1970] suggested this process could lead to auroral arc formation (including, presumably at least the location where the auroral

bulge begins). More sophisticated versions of this ionospheric conductivity feedback mechanism have since been developed [*Lysak*, 1991].

[11] This paper will focus upon the ionospheric conductivity due to the cold (meaning non-magnetospheric) background plasma, although field-aligned conductivity is also required to complete the circuit. In fact these conductivities are initially intimately related, as both depend on the degree of UV insolation. Subsequent development may or may not cause divergence, since field-aligned currents can deplete field-aligned conductivity, while intense aurora creates atmospheric secondaries that resupply both. It is only the initial conditions due to insolation that we will address here. Because initial field-aligned conductivity and ionospheric conductivity are so tightly connected, and because empirical formulas exist for the latter, we will here concentrate on just the ionospheric conductivity. The reader is to understand that the initial field-aligned conductivity also rises and falls with the same seasonal and diurnal patterns. Likewise, because the correlation between the height-integrated Pedersen conductivity and Hall conductivity is r = 0.996, we will here discuss only the Pedersen conductivity. This does not mean that there are any physical grounds for preferring Pedersen conductivity to Hall conductivity.

[12] Resistors in parallel have a total resistance inversely proportional to the sums of the individual inverse resistances. Conductivities in parallel thus add. Because the field-aligned currents required by magnetotail dynamics can flow into either ionosphere, and through a range of local time and latitudes, the global ionospheric conductivity available for current closure can be calculated by simply adding together the conductivity in the two hemispheres, and adding together the conductivity over the appropriate range of latitudes.

[13] We start with the empirical formula for Pedersen conductivity, Σ_P, developed by *Rasmussen et al.* [1988], namely

$$\Sigma_P(\chi) = (4.5/\mathrm{B})\left(1 - 0.85\nu^2\right)\left(1 + 0.15\mathrm{u} + 0.05\mathrm{u}^2\right). \quad (1)$$

[14] We take the magnetic field strength to be B = 0.6 gauss, and the parameter u = F10.7/90 is set at a constant 1.22. The zenith angle, χ, defines ν, namely $\nu = \chi/90$. Equation (1) was derived based on fitting data between $0 \leq \chi \leq 85°$. Past work by our team strongly suggests the formula can be extended down to $\Sigma_P = 0$ ($\chi = 97.6°$). At any rate, arbitrarily setting $\Sigma_P = 0$ at a zenith angle of 85° is physically inaccurate and produces poorer quality fits to auroral luminosity data [*Shue et al.*, 2001]. Until an empirical formula with a greater range of validity exists, we must make do with this one.

[15] The significant current systems (Region 1 and Region 0, associated with the substorm bulge) lie between about 70° and 80°. We thus implicitly assume that the lower latitude R2 currents are not directly involved in magnetotail dynamics, although there is very little nightside conductivity from solar illumination at R2 latitudes anyway. To calculate the average conductivity, patches of size 1 hour in MLT by 1° in MLAT were considered. The conductivity at the middle of each bin was estimated from equation (1) at the midpoint of the bin, for positive and negative MLAT values (Northern and Southern Hemisphere). The conductivity was then averaged over the range $2100 \leq \mathrm{MLT} \leq 0300$, and $70° \leq \mathrm{MLAT} \leq 80°$. Two additional correction were made to equation (1). The solar UV flux varies inversely as the distance from the Sun, hence we multiplied $\Sigma_P(\chi)$ by $(\langle r \rangle / r)^2$, where r = Earth-Sun distance (this produces about a 7% variation from aphelion to perihelion). Second, we weighted each MLAT × MLT grid bin by the factor sin(MLAT), to account for the varying physical surface area of each grid element. (The magnetic coordinate system used was the Altitude Adjusted Corrected Geomagnetic coordinates).

[16] Figure 1 shows the result of this calculation. The absolute values are largely arbitrary (because extending the grid to lower latitudes contributes no additional nightside conductivity, but reduces the mean conductivity by raising the number of grid elements averaged over). The overall pattern, however, is extremely robust, showing very little sensitivity to the exact assumptions made. Extending the MLAT range up to 85° only slightly changes the numbers, slightly reducing the correlations that follow. Extending the MLAT range to 60° has little effect on the correlations. Likewise, the range of MLT covered around midnight matters little. The basic pattern is simply a reflection of when (or if) at least one of the nightside ovals is sunlit. In fact the very simple approach taken by *Lyatsky et al.* [2001] of simply calculating the solar zenith angle at a single point, namely midnight and 70° MLAT, in whichever hemisphere is more sunlit, produces a rough approximation to the conductivity pattern. (Note, however, that conductivity is not linearly related to solar zenith angle, as equation (1) shows).

[17] The seasonal and diurnal variation of global conductivity matches well to the seasonal and diurnal variation of the Am and AL indices. The Am indice is a three-hour range index of geomagnetic activity from midlatitude stations [*Mayaud*, 1980]. Mayaud introduced Am to correct certain deficiencies in Kp. For present purposes the significant distinctions between Am and Kp are that (1) Am includes some geomagnetic stations from the Southern Hemisphere, while Kp uses only Northern Hemisphere stations, and (2) The derivation of Kp is intended to subtract out diurnal variations (under the incorrect assumption that they entirely represent the local time variation of the geomagnetic stations used), (3) The derivation of Kp partially eliminates real seasonal variations [*Mayaud*, 1980, p. 52]. The unfortunate effect is that real geophysical variations in magnetospheric activity are partially removed.

[18] Figure 2 shows the Am pattern of UT/seasonal variation [*Cliver et al.*, 2000; *Lyatsky et al.*, 2001]. Because Am, like Kp, has a resolution of 3 h, the derivation of Figure 2 required interpolation to produce a value for all 24 hour bins. The diurnal variation is actually somewhat larger around the solstices than around the equinoxes (the opposite pattern as for the original Russell-McPherron effect). Specifically, Am has a 24% daily variation in March, and a mere 11% daily variation in September. In June the daily variation is 23%, while in December the daily variation is 37%. Thus averaged over the two solstices, the daily variation is 30%, while averaged over the two equinoxes the daily variation is just 17%.

[19] In June, Am has a minimum at 1500–1600 UT, when the nightside oval is roughly over Siberia and sunlit, while Am is somewhat larger when the nightside oval is

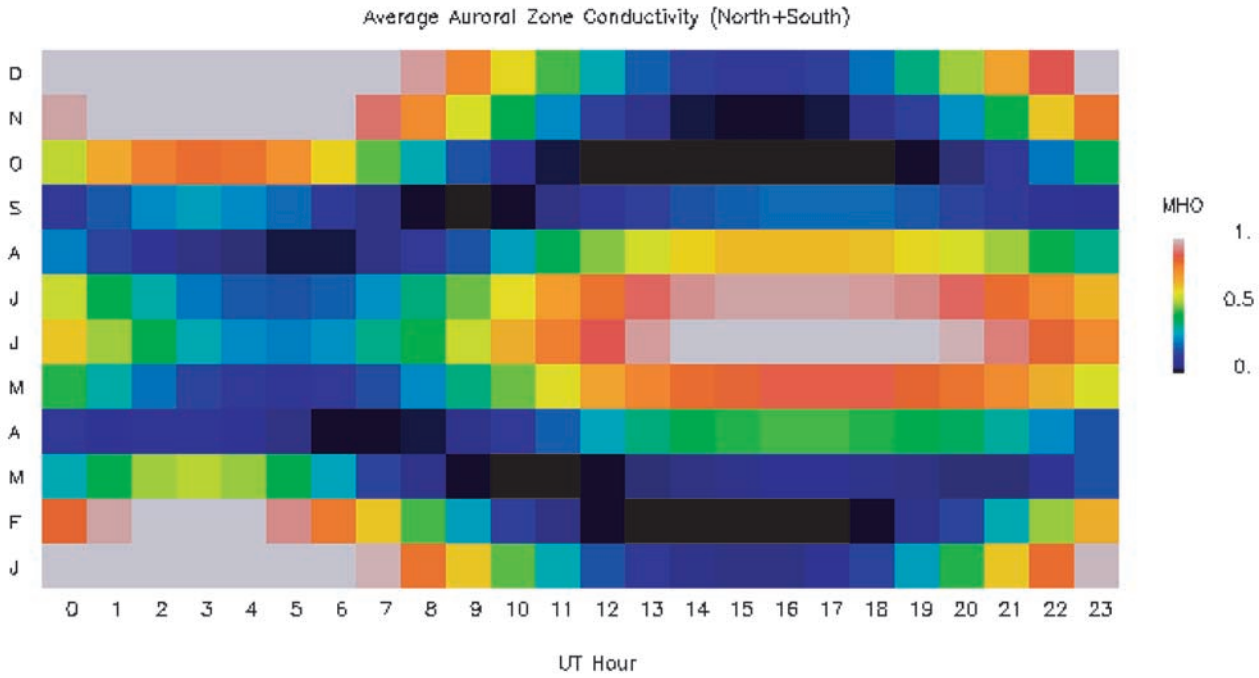

Figure 1. Height-integrated Pedersen conductivity expected from UV insolation of the nightside oval, as a function of month and UT (in hours). Northern and Southern Hemisphere conductivities are combined.

over North American, and in darkness. Likewise, the UT peak for Am in December and January occurs when the Southern Hemisphere oval is in darkness, around 1500 UT. (Of course, the winter hemisphere nightside oval is always in darkness, hence the solstice UT variations are controlled by the insolation in the summer hemisphere). The correlation coefficient between the conductivity pattern as presented in Figure 1 and Am is r = 0.89. Even fairly large variations in the parameters used for the conductance calculations change that number only by about ±0.01. The parameters actually used in Figure 1 are not the optimal fit, but are typical, and seem physically reasonable.

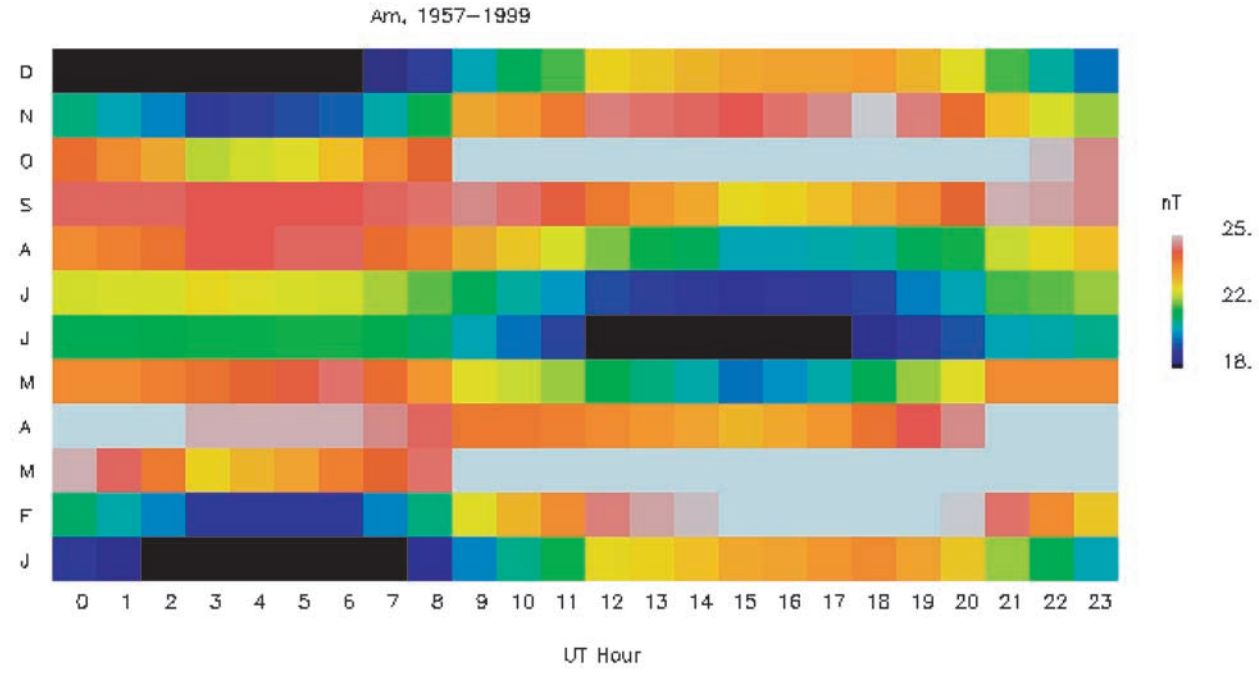

Figure 2. The seasonal and diurnal variation in the Am index.

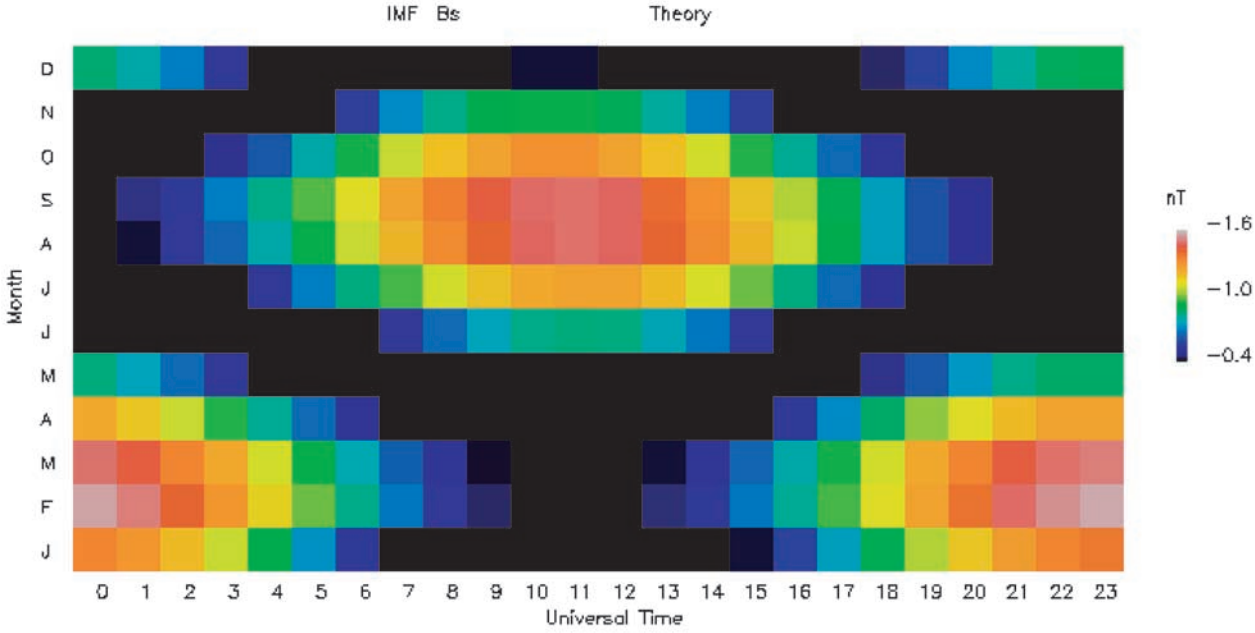

Figure 3. The predicted seasonal and diurnal variation in Bs (IMF GSM B_z when negative, 0 otherwise).

[20] The correlation with the seasonal/diurnal AL patterns is also fairly good, namely r = 0.75. Note however that this means that conductivity effects are accounting for only about half of the AL variations. It is quite possible the lower correlation between AL and Pedersen conductivity arises primarily because of the sparseness of the AL contributing station network – only 12 geomagnetic stations are used, all in the Northern Hemisphere. Indeed, *Ahn et al.* [2000] have argued that the UT variations in the AL indice arise primarily from the spatial distribution of the AL stations. If a significant portion of the seasonal or diurnal effects in AL arises from the inadequate distribution of stations, as *Ahn et al.* [2000] found, the correlation with conductivity will be correspondingly reduced. Nonetheless, it is clear that most of the seasonal and diurnal variations of Am, and a significant portion of AL, can be accounted for by changes in solar insolation of the nightside oval.

3. Generalizing the Russell-McPherron Effect

[21] The solar wind input into the magnetosphere varies with season and with UT because of geometrical considerations involving the Earth's orbit and spin, and the tilt of the Sun's spin axis. This is true even if the solar wind and IMF emerging from the Sun is steady. We now examine seasonal and diurnal variations which arise from the Earth's motion with respect to the Sun in more detail than has been previously considered.

3.1. Seasonal and Diurnal Variations in Bz

[22] *Russell and McPherron* [1973] pointed out that as the Earth rotates around the Sun, the Parker spiral values of the IMF in GSE coordinates remain largely unchanged (except for the tilt of the Sun's spin axis), but the GSM value of B_z changes more significantly. The seasonal and diurnal variation of GSM Bs (= B_z for southward IMF, and = 0 for northward IMF) is shown in Figure 3. In calculating Figure 3, a Parker spiral angle of 45° was assumed. In addition the IMF magnitude was taken to be 10 nT at 1 A.U., to vary inversely as the square of the Earth-Sun distance, and to be independent of heliographic latitude in accordance with the Ulysses observations [*Smith and Balogh*, 1995]. We believe that the present paper is the first to incorporate the variation in the IMF due to the ellipiticity (ε = 0.0167) of the Earth's orbit. This orbital variation creates a variation of about 7% in IMF magnitude between aphelion and perihelion. (Incidentally, *Lyatsky et al.* [2001] showed a version of Figure 3 that also neglected the 7.25° tilt of the Sun to the ecliptic. The effect of the Sun's tilt is to shift the peak values of Bs away from the equinoxes, e.g., to April instead of March. Accounting for variation in the Earth-Sun distance, as is done in this paper, shifts the peak back toward equinoxes and earlier). For the convenience of the reader, we briefly list in one place the full set of assumptions used in calculating Figure 3:

Assumption 1: (Geometrical and astronomical). Sun's spin axis is tilted at 7.25° toward the position the Earth occupies on September 8. The Earth's spin axis is tilted at 23.45°, with perihelion on January 3. The magnetic dipole axis is offset by 9.1°, located at the position given by IGRF 1990. The Earth's motion is elliptical, calculated from standard astronomical formulas.

Assumption 2: (Magnetic fields). The Sun's magnetic field is assumed to be azimuthally symmetric in a coordinate system with the z axis aligned with the Sun's spin axis, and to have no z-component in that system. The field is assumed to have a Parker spiral angle of 45° at a distance of 1 A.U., and to have its magnitude vary with the square of the Earth-Sun distance. The entire IMF structure is tilted into the direction of the Sun's spin axis. Both possible

polarities were averaged over in Figure 3, and in all subsequent figures involving the IMF. By averaging over both polarities, it is physically assumed that the polarity is random and changing, independent of heliographic latitude or other variables.

[23] *Rosenberg and Coleman* [1969] showed that the polarity does depend slightly on heliographic latitude. We did not include this relatively small effect in our calculations. A primary reason for not doing so is that the preferred polarity reverses every 11 years, and hence averages to zero over a 22-year period. Still, for certain purposes such as space weather forecasting, it might be desirable to incorporate the effect reported by *Rosenberg and Coleman* [1969].

[24] The best comparison with Figure 3 can be found in the work of *Cliver et al.* [2000] (again), who calculated the monthly average value of Bs over a 35-year span (their Figure 5a). Although they do not mention it in the text, their results show that from 1963–1997 the highest monthly value of Bs occurred in February, while the smallest month value occurred in July. About a 25% difference exists from peak to trough in the Bs data of *Cliver et al.* [2000]. Our theoretical calculation above predicts the largest Bs value in February, but the smallest value in June, with a peak/trough ratio of 124%, which is much larger than is observed. Of course, numerous solar wind effects such as stream-stream collisions also contribute to the purely geometrical *Bs* calculated here, and perhaps dominate it. (Incidentally, the unremarked upon but extraordinary finding by *Cliver et al.* [2000] of Bs peaking in February over a 35-year period inspired the lead author of the present paper to investigate the Russell-McPherron effect, and its possible generalizations.)

[25] The correlation of Bs with *Am* is r = −0.17, while the correlation with *AL* is r = 0.03. These numbers simply quantify what should be apparent from inspecting Figures 2 and 3, namely, that the expected seasonal and diurnal variations of *Bs* explain relatively little of the seasonal variation in *Am* and *AL*. Indeed, the addition of information on the *Bs* adds essentially nothing to understanding the seasonal and diurnal variation of *Am* and *AL*. Thus the multiple correlation of *AL* and *Am* with Σ_P and *Bs* simultaneously is 0.76 and 0.89 respectively (as opposed to 0.75 and −0.89 with the Pedersen conductivity alone).

3.2. Seasonal and Diurnal Variations in E_{KL}

[26] Almost three decades have passed since *Russell and McPherron* [1973] wisely called attention to the possible seasonal variations in *Bs*. Over that time, research has shown that the behavior of the magnetosphere correlates better with that portion of the solar wind electric field that is associated with magnetospheric-IMF merging. Thus theoretical considerations favor IMF-magnetosphere coupling functions [*Perreault and Akasofu*, 1978; *Kan and Lee*, 1978; *Vasyliunas et al.*, 1982] such as:

$$E_{KL} = vB_T \sin^2(\theta/2) \quad (2)$$

[27] Here E_{KL} is the Kan-Lee electric field, v the solar wind velocity, $B_T = (B_y^2 + B_z^2)^{1/2}$, and $\theta = \tan^{-1}(B_y/B_z)$. (The GSM system is used throughout, unless otherwise specified). The exact formulation for the solar wind input due to merging varies modestly from theorist to theorist (for example, Vasyliunas includes a $p^{-1/3}$ factor, where p is the solar wind dynamic pressure); however, the general theoretical agreement is substantial. Observationally, E_{KL} is also well supported as a good measure of solar wind input. Several studies including such characterizations of the magnetosphere as polar cap potential [*Wygant et al.*, 1983] and auroral luminosity [*Liou et al.*, 1998] favor a solar wind-magnetosphere coupling function such as equation (2). Thus it is well worth considering the seasonal/diurnal variation of E_{KL}. Figure 4 shows that variation.

[28] The assumptions made about the magnetic field are the same as for Figure 3, listed above as assumptions 1 and 2. The solar wind velocity was assumed to not have any radial dependence. This is in accordance with the standard Parker model of the solar wind, in which $v \sim (\log(r/r_c))^{1/2}$, producing a tiny gradient near 1 A.U (r_c is the coronal radius).

[29] On the other hand, v does depend on heliospheric latitude, rising with distance from the Sun's equator, reaching about 800 km/s at midlatitudes and above. *Zieger and Mursula* [1998] have shown that the amplitude of the annual variation seen near-Earth is about 30 km/s. We thus used a simple approximation to represent these empirical effects, namely:

Assumption 3: The solar wind velocity varies with heliographic latitude according to:

$$v = 450. + 350.*|\sin(\Lambda)| \quad (3)$$

where Λ is the Earth's heliographic latitude. Over the narrow range of heliospheric latitude covered by the Earth, equation (3) assumes a nearly linear dependence.

[30] The clear minimum in the Kan-Lee electric field observed in June and July arises in part because the Earth is furthest from the Sun around July 3, and in part because of the heliographic latitude effect. Note that the largest values for E_{KL} again occur in February and March.

[31] The generalized Russell-McPherron seasonal/diurnal variation presented here does modestly improve the fit to the geomagnetic activity indices. Specifically, the correlation of E_{KL} with *Am* rises to r = 0.42, which no longer can be regarded as trivial. Nonetheless, it is still clear that Σ_P, with its 0.89 correlation is by far the better. (E_{KL} correlates only as r = −.05 with AL, versus r = 0.75 for Σ_P). However, geomagnetic activity is not necessarily the totality of magnetospheric response to solar wind driving. As we show in the next section, the seasonal and diurnal variation of certain other magnetospheric state variables may evince a better correlation with E_{KL} than with Σ_P.

[32] Probably the most striking difference between the seasonal/diurnal variation of E_{KL} and that of *Bs* is that the former shows very little diurnal variation (typically about 0.5%, which is too small to be evident on the plots). Since the cone angle obviously does change over the course of a day, this approximate invariance probably deserves some explanation. E_{KL} depends on B_y as well as B_z, and therefore some partial conversion of B_y to B_z naturally produces a less dramatic effect on E_{KL} than on Bs. Nonetheless, it is well worth noting that for either given sign of IMF sector structure, E_{KL} does vary with UT – in fact by as much as 50%. The comparative invariance arises when the two contrasting sector structures are averaged together. Specifically, consider a day and hour such that the Sun's spin tilt creates a negative B_z (even in GSE coordinates), and such

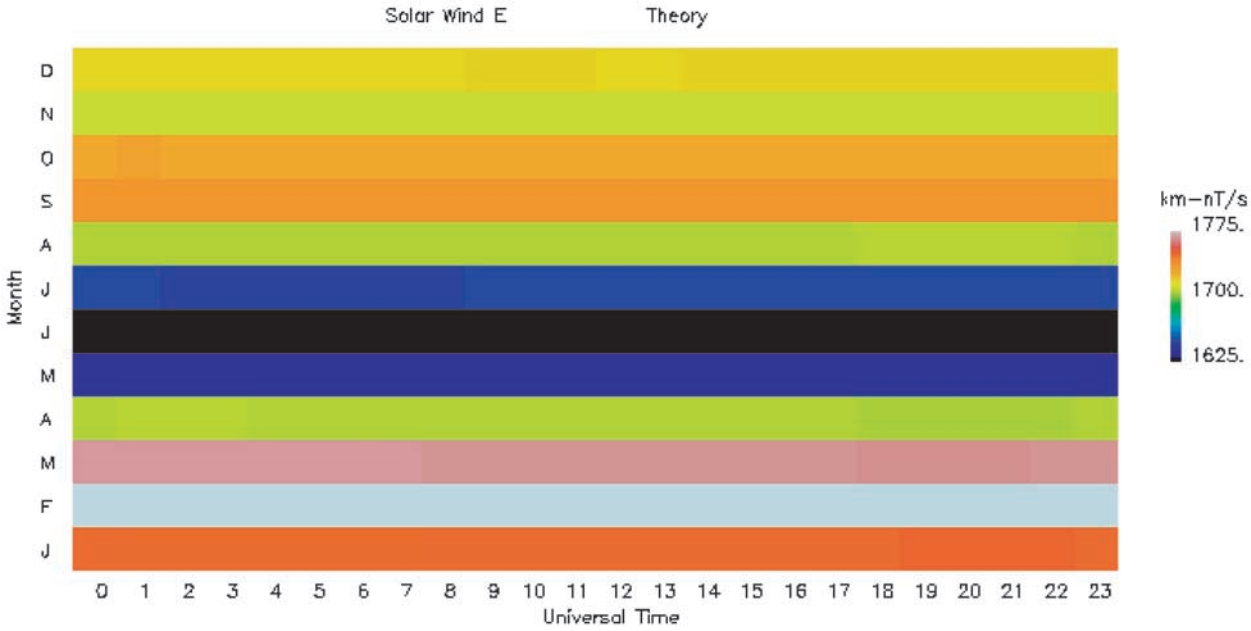

Figure 4. The seasonal and diurnal variation predicted for E_{KL}, the portion of the solar wind associated with merging with the Earth's magnetic field. This variation represents a generalization of the Russell-McPherron effect (shown in Figure 3).

that the Earth's dipole tilt converts some of GSE B_y into negative GSM B_z. That specific UT will thus have a maximum for that sector structure sign. However the opposite sector structure sign will at the same day and hour have a GSE B_z which is positive, and the Earth's dipole axis tilt will result in added positive GSM B_z, creating a minimum at that same hour. Adding together the two opposite signs of sector structure therefore adds the local maximum to the local minimum, leaving relatively little diurnal variation.

[33] By contrast, the Bs calculation assumes a pure half-wave rectifier effect. A positive B_z counts as zero, no matter how positive. A large negative B_z for one sector structure sign is thus not cancelled by a large positive B_z for the other sign; instead Bs is simply cut in half. Thus averaging over both sector structures only modestly reduces the Bs UT variation, while it virtually eliminates the E_{KL} UT variation.

4. Seasonal and Diurnal Variation of Polar Cap Size and Magnetotail Stretching

[34] The state of the magnetosphere is often considered solely in terms of variations observed by magnetic observatories on the surface of the Earth (e.g., Kp, AE, Dst, Am, etc.). This is not because the state of the magnetosphere is necessarily fully or even best expressed subject to such limitations. The long duration and continuous availability of geomagnetic indices simply have no traditional rival. Alternate characterizations of the state of the magnetosphere over a period of many years simply do not exist.

[35] The 18-year span of DMSP creates the potential for introducing additional magnetospheric state variables. Specifically, we have previously advocated b2i, an index of magnetotail stretching [*Sergeev et al.*, 1993; *Newell et al.*, 1998] and polar cap area as important characterizations of the magnetosphere. Both, for example, correlate extremely well with global power associated with auroral luminosity as determined from Polar UVI [*Newell et al.*, 2001], indeed, far better than do any solar wind input functions.

4.1. Magnetotail Stretching Index (b2i) Seasonal and Diurnal Variations

[36] In a stretched magnetotail, high-energy ions are pitch angle scattered as they cross the current sheet, which continuously refills the loss cone. Thus the b2i proxy of magnetotail stretching measures the lowest latitude for which 3–30 keV ions are observed precipitating. b2i correlates extremely well (r = 0.9) with geosynchronous (specifically, the GOES satellite) observations of the magnetotail magnetic field inclination angle [*Newell et al.*, 1998].

[37] We calculated the seasonal and diurnal variation of b2i over the 16-year span 1984–1999 (inclusive). The results are shown in Figure 5. Only those measurements of b2i that have an estimated error of less than 0.5° MLAT were included in the calculation (T. Sotirelis, unpublished work, 2001). For reference, a b2i value of 67° statistically corresponds to Kp = 1, while b2i = 60° corresponds to Kp = 4+ [*Wing and Newell*, 2000]. The equinoctial preference for a stretched magnetotail is readily apparent in Figure 5. Interestingly, the diurnal effects are far more muted than is the case for Am and AL. Perhaps as a result, the correlation with Σ_P is weaker, namely r = 0.38. However, the correlation with E_{KL} is much higher than was the case for the geomagnetic indices. Specifically E_{KL} correlates at the −0.57 level with b2i. Although not as impressive as the Am-Σ_P correlation, it is clearly noteworthy that the E_{KL} -b2i correlation is actually stronger than the Σ_P -b2i correlation. As will be discussed in section 5, one might infer that certain variables characterizing the state of the magneto-

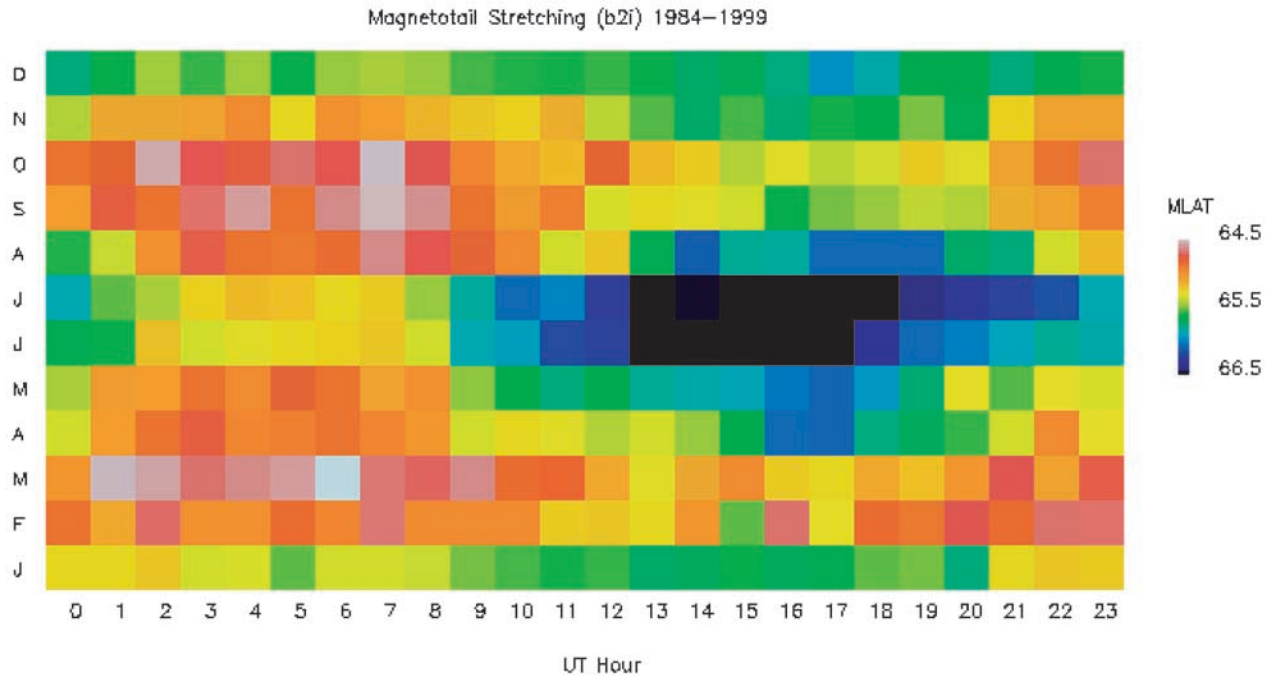

Figure 5. The seasonal and diurnal variation in b2i, the magnetotail-stretching index, from 1984–1999.

sphere behave differently than do high and midlatitude geomagnetic indices.

4.2. Polar Cap Flux (Φ_{PC}) Seasonal and Diurnal Variations

[38] We believe it is possible to identify the open/closed boundary reasonably accurately from low-altitude satellite particle data, which contains detailed spectral resolution, and is making measurements in situ with good spatial resolution. Identifying boundaries with global UV imagers has been a more problematic issue. However because of the poor time resolution of determining the polar cap boundary from DMSP, we have cross-calibrated the Polar UVI auroral boundaries to the DMSP boundaries (J. Carbary, unpublished work, 2001). The result is a determination of the geomagnetic flux (in MWb) threading the open polar cap calibrated to DMSP particle boundaries but with the high time resolution and global coverage of the Polar UVI imager.

[39] Figure 6 shows the seasonal and diurnal variation in polar cap size over a 3-year period as observed by Polar UVI. Again, the state of higher magnetospheric disturbance (larger polar cap size) occurs around the equinoxes. However, more UT variation is noticeable than in the b2i case. The correlation between Σ_P and Φ_{PC} is -0.43, while the correlation between E_{KL} and Φ_{PC} is 0.27. (For reference, Bs correlates at the 0.09 level with Φ_{PC}). No one variable or combination of variable adequately accounts for the seasonal/diurnal variation in Φ_{PC}, but Σ_P does best.

5. Discussion

5.1. Solar Cycle Effects

[40] As previously discussed, the solar wind velocity, v, as observed near Earth, has an annual variation with equinoctial peaks. This variation is clearly due to the corresponding variation in heliospheric latitude of the Earth. The amplitude of the variation however itself varies over the course of a solar cycle. *Zieger and Mursula* [1998] have shown that near solar minimum the amplitude of the annual variation hits a peak of about 50 km/s, or about 11% of the mean solar wind velocity. (For the purposes of calculating the theoretical E_{KL} variations in Figure 4, the seasonal v variation we used, given as equation (3) above, gives an intermediate amplitude of ~30 km/s).

[41] *Zieger and Mursula* [1998] also demonstrated that the solar wind velocity variations are not necessarily symmetric about the heliospheric current sheet. (It may be more accurate to infer that the heliospheric current sheet is in fact displaced from the heliospheric equator. *Crooker et al.* [1997] do in fact reach this conclusion.) Because of this asymmetry of the heliospheric current sheet, the average solar wind velocity can be higher at northern heliographic latitudes during some solar cycles and higher at southern heliographic latitudes during other solar cycles. *Zieger and Mursula* [1998] thus find a spring/fall asymmetry in solar wind velocity at Earth, which reverses sense after each solar maximum. (The amplitude of the yearly variation minimizes at solar maximum). Recall, however, that the total solar wind velocity annual variation amplitude from peak-to-trough is typically less than 10%. Solar cycle variation in the spring/fall v ratio represents another perturbation from the annual undulation. It seemed unnecessary to try adding this second order effect to an already relatively small effect here. Of course, averaged over more than one solar cycle, the spring and fall have equal amplitudes of solar wind velocity.

5.2. Conflict Between Low and High Time Resolution Solar Wind–Magnetosphere Coupling Formulas

[42] *Crooker et al.* [1977] reported half-yearly averages of solar wind v and Ap (the latter is a minor variant of the

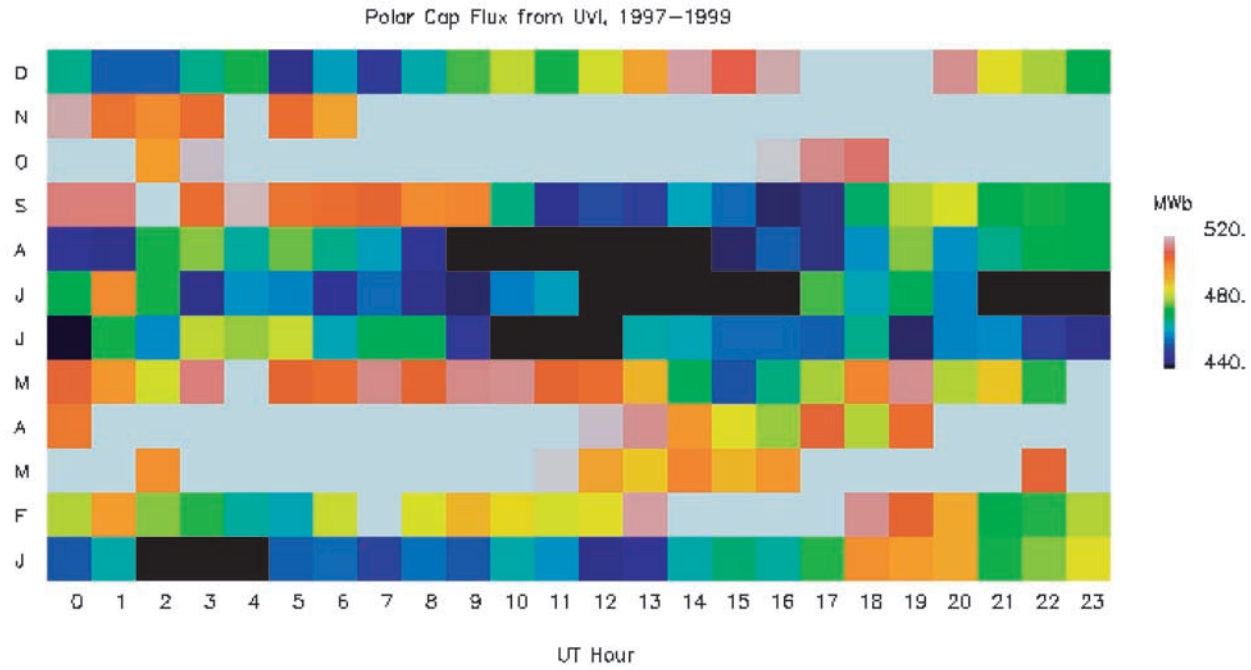

Figure 6. The seasonal and diurnal variation in Φ_{PC}, the polar cap flux. The size of the polar cap is taken from Polar UVI observations from 1997–2000.

Kp index) were highly correlated during solar cycle 20. However, *Crooker and Gringauz* [1993] reported a breakdown in that linear relationship beginning with solar cycle 21. Over a longer time interval, *Crooker and Gringauz* [1993] reported that Ap correlated better with Bsv^2. Several other researchers using data with similar time resolution – half yearly – have reported similar results, with minor variants. For example, *Ahluwalia* [2000] used half-yearly solar wind averages to find a good correlation with Bv^2 (i.e., total B rather than Bs).

[43] On the other hand, a great deal of theoretical [*Perreault and Akasofu*, 1978; *Kan and Lee*, 1978; *Vasyliunas et al.*, 1982] work suggests that solar wind-magnetosphere coupling should depend linearly on the velocity. Observational work at higher time resolution (varying from 1 minute through 1 hour) [*Wygant et al.*, 1983; *Liou et al.*, 1998] has also consistently supported a linear dependence of parameters such as cross-polar cap potential and auroral luminosity on v. Why then the discrepancy between low and high time resolution data?

[44] We believe that at the half-yearly or yearly resolution, experimenters are in fact exploring solar cycle variations more than magnetospheric–solar wind coupling. The variations in v over such a long timescale may serve mainly as a proxy for solar cycle phase. For example, solar UV insolation, the magnitude of v and B and especially their standard deviations, all change over the course of a solar cycle. The variation in solar UV flux (F10.7), for instance, can also be treated as an indicator of solar cycle phase, and is not necessarily causally related to all variables with which it linearly correlates. The same must be true of v.

[45] On the other hand, the physics of magnetosphere-ionosphere interaction are probably invariant over a wide range of timescales. Investigations performed over a period of hours, days, or even weeks experience little change in solar cycle phase. These higher time resolution measurements should therefore be representative of the true dynamic relationship between variables. Thus we believe high time resolution studies to be more authoritative than are the low time resolution studies, and accordingly rely on a linear dependence on v in calculation solar wind input in this paper (E_{KL}).

5.3. Observed Dependence on Σ_P or E_{KL}

[46] Both Σ_P and E_{KL} represent solar inputs. The former represents UV insolation, while the latter represents the likely electromagnetic coupling of the solar wind to the magnetosphere (specifically that due to merging). We believe the evidence of the last 4 decades or so of magnetospheric research adequately establishes the leading role of solar wind input as the most important driver of magnetospheric dynamics. Yet the solar wind input has only relatively small systematic seasonal and diurnal variations (about 14% and 0.5% respectively), while solar insolation of the nightside auroral oval is far more variable. Since UV insolation of the nightside oval also varies more greatly and systematically with season and UT, it is logical that insolation is the solar input that is responsible for most of the seasonal and diurnal variation in magnetospheric or ionospheric response.

[47] It is well worth collecting together in one table the correlations of the 4 dependent variables considered here – Am, AL, b2i, and Φ_{PC}, as is done in Table 1. AL, representative of the nightside auroral electrojet, correlates best, by far, with Σ_P, as does Am, which is representative of general geomagnetic activity. The polar cap flux has a weaker correlation, but it is still best with Σ_P. Finally the magnetotail stretching proxy, b2i, is the sole variable tested

Table 1. Correlations Between Various Patterns of Seasonal and Diurnal Variations[a]

	Σ_P	Bs	E_{KL}
Am	**−0.89**	−0.17	0.42
AL	**0.75**	0.03	−0.05
Φ_{PC}	**−0.49**	0.12	0.35
b2i	0.38	0.26	**−0.57**

[a] Four characterizations of the magnetosphere state are given in the left column. The three dependent variables are the height-integrated global nightside Pedersen conductivity from insolation, and two model solar wind input variables. The best correlation is given in boldface.

here whose seasonal and diurnal variations correlate best with the solar wind input.

[48] Of the two solar wind input variables considered here, namely Bs and E_{KL}, the latter correlates better with all 4 magnetosphere/ionosphere state variables. Indeed, it can be safely said that Bs does *not* correlate significantly with any state variable, except possibly magnetotail stretching, where it still explains less of the variation than does E_{KL}.

[49] One may also invert the question, and consider which state variables have the highest correlation. Am correlates much better with all three independent variables than does AL. We do not believe this means that the physical auroral electrojet is less responsive to solar inputs than is midlatitude geomagnetic activity. Rather, we believe that Am is a more accurate measure of geomagnetic activity than AL is of global auroral electrojet activity. Mayaud designed Am to include data from an adequate number of geomagnetic ground stations in both hemispheres. AL includes data only from the Northern Hemisphere, and even there only from 12 imperfectly distributed stations. Because of its more global coverage, Am is better able to capture the specific type of geomagnetic activity it was designed to represent.

[50] The situation is different with the magnetospheric state variables b2i and Φ_{PC}. Although measured from low-altitude Earth orbit, these variables in fact represent the state of the magnetosphere and not specifically the ionosphere. Thus we believe the finding that the magnetotail stretching index, b2i, correlates better with E_{KL} than with Σ_P probably accurately represents the physics of the magnetotail.

[51] Finally, we should note that the correlation between the global Pedersen conductivity, introduced in this paper, and the traditional variable associated with unspecified equinoctial (McIntosh) models, ψ, is surprisingly high (at any rate, the present authors were surprised). ψ is defined as the acute angle between the Earth's dipole axis and the Earth-Sun line. *McIntosh* [1959] noted many years ago that the seasonal variation appeared to correlate well with ψ. Although it is apparent that only one nightside oval (at most) can be sunlit, and that this will happen best when one dipole axis is tilted toward the Sun, it surprised the present authors to learn that the correlation between Σ_P and ψ is 0.98 (in fact 0.985 rounded to three decimal places). However, the *McIntosh* [1959] ψ variable is not a physical model, as is the conductivity effect, and thus we believe the latter conceptually superior even though difficult to distinguish in practice. The fact that intense aurora and intense field-aligned electric fields (along with auroral kilometric radiation, etc.) are observed in the winter hemisphere and not the summer hemisphere further supports the value of the conductivity model as supplying the missing physics behind the McIntosh 'model'. For reference, the correlations of ψ with the seasonal and diurnal variations of Am and AL are 0.89 and −0.73 respectively.

[52] Finally, we note that *Orlando et al.* [1995] has previously correlated a version of the equinoctial model with Am. Specifically *Orlando et al.* [1995] correlated $\cos^2(\psi)$ rather than ψ, reporting a significantly lower correlation coefficient (53% of the variance accounted for, ordinarily implying r = 0.73). The reason for using $\cos^2(\psi)$ was because *Boller and Stolov* [1970] suggested that the Kevin-Helmholtz instability might depend on that variable. However, *Cliver et al.* [2000] reported that the correlation coefficients between ψ and Am to be 0.91, and the correlation between $\cos^2(\psi)$ and Am to be −0.89. Our own findings essentially agree with *Cliver et al.* [2000], although our calculations show correlations that are slightly lower (we find the correlation between Am and ψ to be 0.89, while that between $\cos^2(\psi)$ and Am is −0.88). At any rate, it appears to have been adequately established in the intervening years that merging, not the Kevin-Helmholtz instability, represents the solar wind input that drives magnetospheric dynamics. The key empirical result certainly is the one emphasized by *Cliver et al.* [2000]: Am correlates much better with ψ (or as we show, with Σ_P) than with Bs.

5.4. Expected Dependence on Σ_P or E_{KL}

[53] The effect of increased solar wind input, meaning larger E_{KL}, is to increase the polar cap size and magnetotail stretching. The increased magnetotail current amplitudes and stored magnetic energy density should in turn increase the frequency and size of substorms (increasing Am and AL). Each substorm will partially reduce magnetotail currents, but no contradiction exists. The increased substorm frequency and severity is a consequence of increased magnetotail stretching, and can therefore only partially offset the increased E_{KL}. It is thus straightforward to deduce that E_{KL} should be negatively correlated with b2i (which is smaller for more stretched magnetotail conditions) and positively correlated with Φ_{PC}, Am, and negatively with AL.

[54] The expected relationship between Σ_P and the state variables considered here may be less obvious. It is our hypothesis that those portions of the magnetotail currents which normally close in the sunlit ionosphere are unable to do so when Σ_P is small. We thus expect a small value of Σ_P to be associated with increased magnetotail stretching, and a larger polar cap size. However, this larger amount of stored magnetic energy in the magnetotail occurs under conditions that are less stable. When the nightside oval is dark, any patch of auroral precipitation will create a conducting path for currents to flow, and hence induce more localized precipitation [*Atkinson*, 1970]. The patch then becomes still more conducting, and under certain conditions will induce still more precipitation in a positive feedback loop [*Lysak*, 1991]. The end result is intense auroral activity, perhaps including a substorm auroral bulge. Thus we predict that Σ_P should be negatively correlated with Φ_{PC} and Am, and positively with b2i and AL.

5.5. Observed Solar Wind Input Versus Theoretical Input

[55] The existing literature on solar wind input into the magnetosphere is large, and we do not wish to delve too

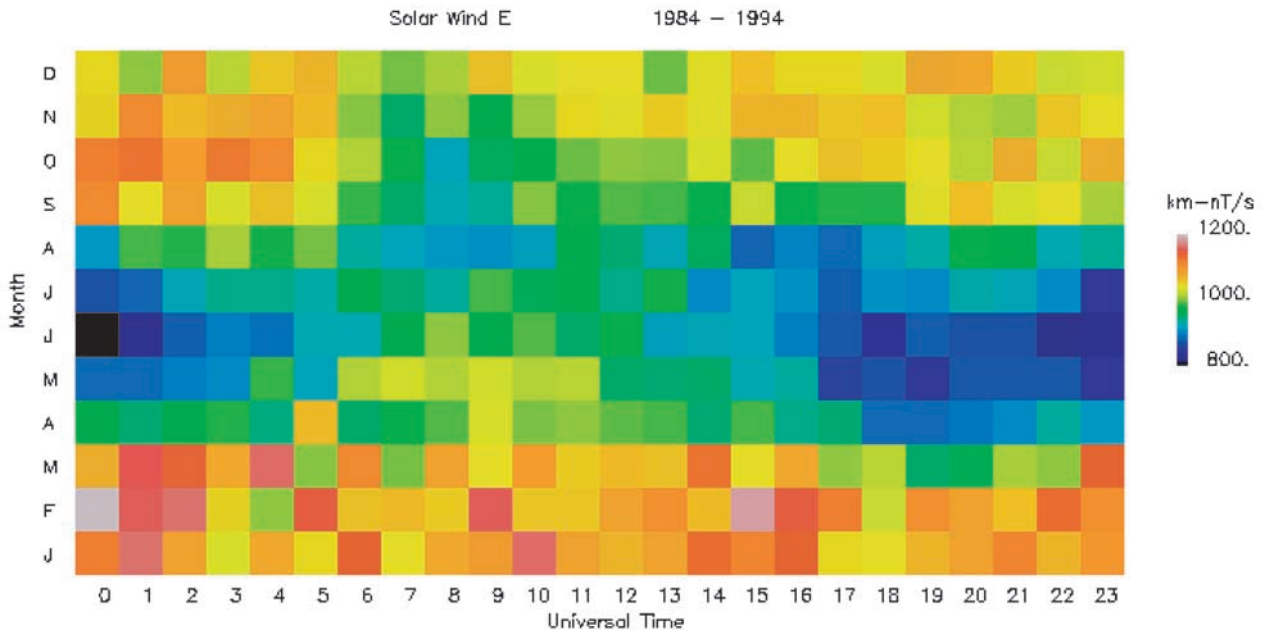

Figure 7. The observed seasonal and diurnal variation in E_{KL}, from 1984–1994.

deeply into the subject. Nonetheless, we feel it incumbent upon us to report how the observed E_{KL} varies with respect to our theoretical predictions. Figure 7 illustrates an 11-year average for E_{KL} calculated from the NASA Goddard OMNI database from 1984–1994 (thus using only the near-Earth IMP 8 data). Besides the advantage of covering one full solar cycle (and hence range of solar wind velocities, and so forth), this time frame excludes data from satellites making excursions as large as 1% of the Earth-Sun distance (about as far as the Earth moves in a day, raising issues of satellite location for proper binning).

[56] A simple nearest neighbor smoothing has been applied to Figure 7, which has a correlation with Figure 4 (the theoretical model) of 0.70. (Prior to the application of the nearest neighbor smoothing, the correlation was only 0.49, indicating the presence of appreciable random fluctuations in the data.) The theoretically predicted June minimum and February maximum are clearly observable.

[57] The observed E_{KL} over the 11 years sampled correlates slightly better with Φ_{PC}, but significantly worse with magnetotail stretching than does the theoretical E_{KL}. Specifically, the observed E_{KL} correlates at the 0.40 and −0.42 level with Φ_{PC} and b2i respectively, while the theoretical variations in E_{KL} correlate with Φ_{PC} and b2i at the r = .35 and r = −0.57 levels. (The correlations with Am and AL are small enough, and the correlations of these geomagnetic indices with Σ_P are so high anyway, it is not worth comparing the observed with the predicted solar wind input variables). It is somewhat unusual for the predicted value of an independent variable to better explain the variation in the system dependent variables than does the actual observed independent variable. It is possible that measurement uncertainties or other effects limit the correlations of the observed E_{KL}.

[58] In any case, the predicted E_{KL} seasonal and diurnal variations presented here are calculated incorporating some very well established principles. The geometrical considerations and the details of the Earth's motion about the Sun are certainly not in doubt. This calculation therefore is well worth doing, even if some new facets of solar wind behavior or a more sophisticated approach in the future improves on what has been done here.

6. Summary and Conclusions

[59] The pattern of seasonal and diurnal variations of Am and AL correlate extremely well – 0.89 and 0.75 – with the corresponding variation in Pedersen conductivity in the nightside oval, Σ_P. The smaller correlation with AL probably stems from UT variations due to the distribution of geomagnetic stations used [*Ahn et al.*, 2000]. Because Σ_P in turn correlates well with the traditional McIntosh variable (ψ, the acute angle between the Earth-Sun line and the Earth's dipole axis) our results involving these geomagnetic variables differ from earlier work [*McIntosh*, 1959; *Cliver et al.*, 2000; *Ahn et al.*, 2000] primarily in that a more concrete physical interpretation provides an explanation the McIntosh effect. Specifically, our work strongly suggests that auroral and geomagnetic activity depends on solar UV input as well as on solar wind input. We note again that the same results follow from using the Hall conductivity instead of the Pedersen conductivity. Because the correlation between these latter two variables is so high (r = 0.996), it would be redundant to use both in our investigation.

[60] The more original parts of our paper lie elsewhere. We have here generalized the seasonal and diurnal variations in solar wind input arising from the orbital and spin motions of the Earth (the Russell-McPherron effect). Specifically, we considered the seasonal and diurnal variation of E_{KL}, which is widely believed to be a better measure of the merging electric field than *Bs* alone. In doing so, we considered certain elements of seasonal variation, such as that due to variation in the Earth-Sun distance, which have

been generally neglected (we have thereby explained the February peak in *Bs*, which is clearly observable over a 35-year period). This generalized Russell-McPherron seasonal variation in solar wind input shows different properties than the original. In particular, (i) E_{KL} has very little UT variation (0.5%); (ii) E_{KL} peaks in February, (iii) E_{KL} has a minimum in June. However, the amplitude of the seasonal variation is only about 14%, as opposed to the much larger variations observed in AL and Am. Although E_{KL} does correlate better with the seasonal and diurnal variations in Am and AL than does Bs, it still does not correlate nearly so well as does Σ_P.

[61] We believe that we are the first to study the dependence of magnetospheric state variables that do not rely on geomagnetic observatories. Certainly, we are the first to investigate the seasonal and diurnal variations in polar cap size, Φ_{PC}, and in the magnetotail-stretching index, b2i. These variables have only a very indirect relationship with auroral activity. It is therefore not obvious that they should display just the same behavior as the geomagnetic indices. In fact, the magnetotail stretching index, b2i, proves to have a higher correlation, -0.57, with E_{KL} than with Σ_P. However, Φ_{PC} correlates better with Σ_P (-0.49) than with solar wind input variables.

[62] We conclude that the seasonal and diurnal variations in magnetotail stretching is driven directly by corresponding variations in the solar wind input arising from orbital and spin motions of the Earth (i.e., by the generalized Russell-McPherron effect introduced here). However geomagnetic activity, at least as represented by AL and Am, owes its seasonal and diurnal variability primarily to variations in solar UV illumination of the nightside auroral oval.

[63] **Acknowledgments.** This work was supported by AFOSR grant F49620-00-1-0172, by NASA grant NAG 5-11350 and by NSF grant ATM-9909258. The DMSP particle detectors were designed by D. Hardy of AFRL, and obtained from JHU/APL. We thank D. Hardy and F. Rich for its use. We also thank G. Parks of U.C. Berkeley, the P. I. on Polar UVI.

[64] Arthur Richmond thanks Byung-Ho Ahn and K. Mursula for their assistance in evaluating this paper.

References

Ahluwalia, H. S., AP time variations and interplanetary magnetic field intensity, *J. Geophys. Res.*, *105*, 27,481, 2000.

Ahn, B.-H., H. W. Kroehl, Y. Kamide, and E. A. Kihn, Universal time variations in the auroral electrojet indices, *J. Geophys. Res.*, *105*, 267, 2000.

Atkinson, G., Auroral arcs: Result of the interaction of a dynamic magnetosphere with the ionosphere, *J. Geophys. Res.*, *75*, 4746, 1970.

Boller, B. R., and H. L. Stolov, Kelvin-Helmholtz instability and the semiannual variation of geomagnetic activity, *J. Geophys. Res.*, *75*, 6073, 1970.

Chamberlain, J. W., *Physics of the Aurora and Airglow*, Academic, San Diego, Calif., 1961.

Cliver, E. W., Y. Kamide, and A. G. Ling, Mountains versus valleys: Semiannual variation of geomagnetic activity, *J. Geophys. Res.*, *105*, 2413, 2000.

Collin, H. L., W. K. Peterson, O. W. Lennartsson, and J. F. Drake, The seasonal variation of auroral ion beams, *Geophys. Res. Lett.*, *25*, 4071, 1998.

Crooker, N. U., and K. I. Gringauz, On the low correlation between long-term averages of solar wind speed and geomagnetic activity after 1976, *J. Geophys. Res.*, *98*, 59, 1993.

Crooker, N. U., J. Feynman, and J. T. Gosling, On the high correlation between long-term averages of solar wind speed and geomagnetic activity, *J. Geophys. Res.*, *82*, 1933, 1977.

Crooker, N. U., A. J. Lazarus, J. L. Phillips, J. T. Steinberg, A. Szabo, R. P. Lepping, and E. J. Smith, Coronal streamer belt asymmetries and seasonal solar wind variations deduced from Wind and Ulysses data, *J. Geophys. Res.*, *102*, 4673, 1997.

Erlandson, R. E., and L. J. Zanetti, A statistical study of auroral electromagnetic ion cyclotron waves, *J. Geophys. Res.*, *103*, 4627, 1998.

Kan, J. R., and L. C. Lee, Energy coupling functions and solar wind magnetosphere dynamo, *Geophys. Res. Lett.*, *6*, 577, 1978.

Kasaba, Y., H. Matsumoto, H. Hashimoto, and R. R. Anderson, The angular distribution of auroral kilometric radiation observed by GEOTAIL spacecraft, *Geophys. Res. Lett.*, *24*, 2483, 1997.

Kumamoto, A., and H. Oya, Asymmetry of occurrence-frequency and intensity of AKR between summer polar region and winter polar region sources, *Geophys. Res. Lett.*, *25*, 2369, 1998.

Liou, K., P. T. Newell, C.-I. Meng, M. Brittnacher, and G. Parks, Characteristics of the solar wind controlled auroral emissions, *J. Geophys. Res.*, *103*, 17,543, 1998.

Lyatsky, W., P. T. Newell, and A. Hamza, Solar illumination as cause of the equinoctial preference for geomagnetic activity, *Geophys. Res. Lett.*, *28*, 2353, 2001.

Lysak, R. L., Feedback instability of the ionospheric resonant cavity, *J. Geophys. Res.*, *96*, 1553, 1991.

Mayaud, P. N., *Derivation, Meaning, and Use of Geomagnetic Indices*, *Geophys. Monogr. Ser.*, vol. 22, AGU, Washington, D.C., 1980.

McIntosh, D. H., On the annual variation of magnetic disturbances, *Philos. Trans. R. Soc. London, Ser. A*, *251*, 525, 1959.

Newell, P. T., New findings about auroras confirm importance of ionosphere in space weather, *Eos Trans. AGU*, *79*, 627, 1998.

Newell, P. T., C.-I. Meng, and K. M. Lyons, Discrete aurorae are suppressed in sunlight, *Nature*, *381*, 766, 1996.

Newell, P. T., V. A. Sergeev, G. R. Bikkuzina, and S. Wing, Characterizing the state of the magnetosphere: Testing the ion precipitation maxima latitude (b2i) and the ion isotropy boundary, *J. Geophys. Res.*, *103*, 4739, 1998.

Newell, P. T., C.-I. Meng, T. Sotirelis, and K. Liou, Polar Ultraviolet Imager observations of global auroral power as a function of polar cap size and magnetotail stretching, *J. Geophys. Res.*, *106*, 5895, 2001.

Orlando, M., G. Moreno, M. Parisi, and M. Storini, Diurnal modulation of the geomagnetic activity, induced by southward component of the interplanetary magnetic field, *J. Geophys. Res.*, *100*, 19,565, 1995.

Perreault, W. K., and S.-I. Akasofu, A study of geomagnetic storms, *Geophys. J.R. Astron. Soc.*, *54*, 547, 1978.

Petrinec, S. M., W. L. Imhof, D. L. Chenette, J. Mobilia, and T. J. Rosenberg, Dayside/nightside auroral X ray emission differences-Implications for ionospheric conductance, *Geophys. Res. Lett.*, *20*, 3277, 2000.

Rasmussen, C. E., R. E. Schunk, and V. B. Wickwar, A photochemical equilibrium model for ionospheric conductivity, *J. Geophys. Res.*, *93*, 9831, 1988.

Rosenberg, R. L., and P. J. Coleman, Heliographic latitude dependence of the dominant polarity of the interplanetary magnetic field, *J. Geophys. Res.*, *74*, 5611, 1969.

Russell, C. T., and R. L. McPherron, Semiannual variation of geomagnetic activity, *J. Geophys. Res.*, *78*, 92, 1973.

Sergeev, V. A., M. V. Malkov, and K. Mursula, Testing of the isotropic boundary algorithm method to evaluate the magnetic field configuration in the tail, *J. Geophys. Res.*, *98*, 7609, 1993.

Shue, J.-H., P. T. Newell, K. Liou, and C.-I. Meng, The quantitative relationship between auroral brightness and solar EUV Pedersen conductance, *J. Geophys. Res.*, *106*, 5883, 2001.

Smith, E. J., and A. Balogh, Ulysses observations of the radial magnetic field, *Geophys. Res. Lett.*, *22*, 3317, 1995.

Vasyliunas, V. M., J. R. Kan, G. L. Siscoe, and S.-I. Akasofu, Scaling relations governing magnetospheric energy transfer, *Planet. Space Sci.*, *30*, 359, 1982.

Wing, S., and P. T. Newell, Quiet time plasma sheet ion pressure contribution to Birkeland currents, *J. Geophys. Res.*, *105*, 7793, 2000.

Wygant, J. R., R. B. Torbert, and F. S. Mozer, Comparison of S3-3 polar cap potential drops with the interplanetary magnetic field and models of magnetopause reconnection, *J. Geophys. Res.*, *88*, 5727, 1983.

Zieger, B., and K. Mursula, Annual variation in near-Earth solar wind speed: Evidence for persistent north-south asymmetry related to solar magnetic polarity, *Geophys. Res. Lett.*, *25*, 841, 1998.

C.-I. Meng, P. T. Newell, J. P. Skura, and T. Sotirelis, Applied Physics Laboratory, Johns Hopkins University, Laurel, MD 20723, USA. (patrick.newell@jhuapl.edu)

W. Lyatsky, Alabama A&M University, Normal, AL 35762, USA.